

Cite this: *J. Anal. At. Spectrom.*, 2011, **26**, 845

www.rsc.org/jaas

PAPER

Precise U–Pb zircon dating at a scale of <5 micron by the CAMECA 1280 SIMS using a Gaussian illumination probe†

Yu Liu,^a Xian-Hua Li,^{*a} Qiu-Li Li,^a Guo-Qiang Tang^a and Qing-Zhu Yin^b

Received 15th August 2010, Accepted 26th November 2010

DOI: 10.1039/c0ja00113a

Zircon is arguably the best, certainly the most commonly used mineral for U–Pb geochronology. Modern large-geometry secondary ion mass spectrometry (SIMS) has been routinely utilized for precise U–Pb zircon age determination at a lateral resolution of 10–30 μm . However, *in situ* U–Pb dating at a scale of *ca.* 5 μm scale or less for fine-grained zircons and/or zircon crystals with complex structural and chemical features is still a challenge to the geoscience community. Here we describe a method of precise U–Pb dating for zircons as young as the Jurassic age at a scale of up to <5 μm using the CAMECA ims-1280 SIMS. Gaussian mode primary O_2^- and O^- probes of *ca.* 5.2 μm and *ca.* 4.5 μm in diameter with beam intensities of ~ 100 pA were obtained, respectively, by optimizing the primary column. Secondary ion optics was optimized to ensure a high Pb^+ sensitivity in zircons, producing ~ 21 cps/ppm/nA using O_2^- and ~ 13 cps/ppm/nA using O^- (with oxygen flooding technique). As a demonstration of this method, three well-characterized zircon standards with a range of ages, AS3 (1099 Ma), Plešovice (377 Ma) and Qinghu (159.5 Ma), were analyzed. We demonstrate with these zircon standards that their ages could be determined with precision and accuracy of 1–2% using a spot <5 micron. The O^- primary beam is preferred over the O_2^- beam for small-spot U–Pb zircon geochronology, because it has higher density and produces smaller craters on the target surface, with insignificant trade off in precision and accuracy of the final U–Pb ages. For U-poor minerals of younger ages, O_2^- might be preferred in order to generate sufficient Pb^+ ions for measurement with minimal loss of spatial resolution.

1. Introduction

Zircon, ZrSiO_4 , is a common U-rich accessory mineral occurring in many types of terrestrial and extraterrestrial rocks. Zircon is the best mineral for geochronology based on the radioactive decay of U to Pb. It has an extremely low initial daughter (Pb) and high parent (U). It is of singular importance in geosciences.¹ Since the inception of *in situ* microanalysis using SIMS (secondary ion mass spectrometry),² high precision and high lateral resolution have been recognized as being amongst the most important requirements for SIMS U–Pb zircon age determinations. Large-geometry, double-focusing SIMS techniques, including SHRIMP (Sensitive High Resolution Ion MicroProbe) and CAMECA ims-1270/1280, are now used routinely for U–Pb geochronology, achieving a U–Pb zircon age precision of *ca.* 1% and a lateral sampling scale of *ca.* 10–30 μm (*e.g.*, ref. 3–5).

Despite great success in addressing many problems in U–Pb zircon geochronology, there is an increasing need to reduce the routine lateral resolution to a scale of <10 μm for the *in situ* analysis of fine-grained zircons and/or zircon crystals with complex structural and chemical features.

Attempts have been made to improve the spatial resolution at a scale of <10 μm in recent investigations by means of three major approaches. One is the direct production of a small primary ion beam (typically <5 μm) using the CAMECA NanoSIMS.⁶ This instrument has a coaxial design incorporating a primary column and a secondary extraction column, making it a unique ion microprobe optimized for high lateral resolution. Using an ellipse primary O^- ion beam spot of ~ 4.5 μm , Stern *et al.*⁶ obtained a $^{207}\text{Pb}/^{206}\text{Pb}$ age of 504 ± 18 Ma for zirconolite ($\text{CaZrTi}_2\text{O}_7$). However, the NanoSIMS has a lower secondary ion sensitivity than the large-geometry SIMS mainly due to its smaller magnet and spherical electrostatic sector analyzer radius. For instance, the sensitivity of secondary Pb^+ in zircon is only 3–4 cps/ppm/nA using O^- ,⁶ in contrast with *ca.* 13–21 cps/ppm/nA using O^- or O_2^- and the CAMECA ims-1280 SIMS (see below). Therefore, a long acquisition time (*ca.* 40 min per analysis) is needed,⁶ and the precision is relatively poor when using the NanoSIMS.

^aState Key Laboratory of Lithospheric Evolution, Institute of Geology and Geophysics, Chinese Academy of Sciences, Beijing, 100029, China. E-mail: lixh@gig.ac.cn; Fax: +86-10-62010846; Tel: +86-10-82998512

^bDepartment of Geology, University of California Davis, One Shields Avenue, Davis, CA, 95616, USA

† Electronic supplementary information (ESI) available. See DOI: 10.1039/c0ja00113a

Another approach is an “indirect” reduction of the analytical area by means of limiting the secondary ion beam on the image plane by partially closing the Field Aperture (FA) of the CAMECA ims-1270 large-geometry SIMS instrument.^{7,8} With a 20–25 μm Köhler illumination primary O^- beam, a secondary ion beam of the same size is projected onto the image plane where the FA is located. By reducing the FA to a certain window size, only the secondary ions coming from the area of interest (smaller than the spot size) are transferred into the spectrometer. While the analytical area is reduced to $<10 \mu\text{m}$ and $\sim 95\%$ of the surface-derived contamination can be removed, the useful signal is simultaneously reduced by $\sim 60\%$. Thus, the ratio of the signals of interest to contaminants is compromised because of the incomplete elimination of contaminants, particularly for dating small minerals surrounded by materials containing high concentrations of Pb.

The third method for overcoming the 2-D spatial selectivity limited by the size of the primary beam in SIMS analyses, typically 10–30 μm , for accessory mineral analysis is using the depth profiling mode of SIMS. This method was successfully applied in the age determination of Th-Pb in monazite⁹ as well as in U-Pb zircon dating.¹⁰ According to this method, a spatial resolution of $\sim 0.2 \mu\text{m}$ can be achieved in the secondary ion axial direction, which is superior to any of the other known methods. In practice, however, the method requires that the mineral grain has to be taken out of the SIMS sample chamber and carefully re-polished by hand prior to depth profiling. This needs to be done under constant examination by a reflected light microscope and profilometer to make sure that the deep crater depth is adequately removed from the previous session. The zircon grain surface is then cleaned and recoated with Au before the next depth profiling session is carried out on the same spot. The cycle has to be repeated many times until the entire depth is probed to the investigator's satisfaction. It is not really an *in situ* method, as it requires the zircon grains to be isolated from rock or thin sections, and the crystal prism needs to be very carefully placed to ensure that the internal growth layers of the crystal align perfectly parallel to the lateral dimensions of the ion beam; otherwise, a mixed age may be obtained. The method is tedious and time consuming.

In this work, we document a new U-Pb zircon age dating method by the CAMECA ims-1280 SIMS using the Gaussian illumination mode of the primary ion beam together with the high transmission of secondary ions, with the aims of achieving precise and accurate (1–2%) U-Pb zircon ages at a scale of $<5 \mu\text{m}$. Our results indicate that zircons as young as the Jurassic age can be precisely and accurately dated at a scale of $<5 \mu\text{m}$ using the method developed in this study.

2. Instrument

All measurements were conducted using the CAMECA ims-1280 SIMS at the Institute of Geology and Geophysics, Chinese Academy of Sciences in Beijing. The CAMECA ims-1280 SIMS is a large-geometry, double-focusing instrument, which has the same radius (585 mm) for both the electrostatic sector analyzer (ESA) and the sector magnet. It is equipped with two primary ion sources (Fig. 1), the Duoplasmatron source which uses oxygen gas and the caesium ion source. The secondary ion optics can be

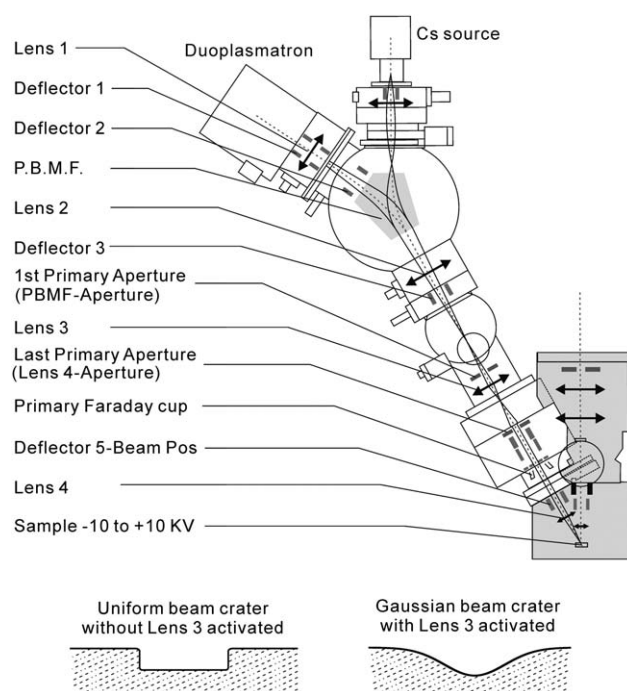


Fig. 1 Schematic diagram of the CAMECA ims-1280 primary column (modified from the CAMECA ims-1280 user's guide), the Köhler beam with uniform density distribution can be obtained without Lens 3, and the Gaussian beam density distribution can be obtained with Lens 3 activated.

optimized to work at almost full transmission up to 6000 mass resolving power (MRP). The Köhler illumination primary beam of O^- or O_2^- with lateral resolution of 10–30 μm is normally used for U-Pb zircon measurement. Here we show that the Gaussian primary beam size could be reduced to $<5 \mu\text{m}$, and meaningful U-Pb age could be determined.

3. Analytical methods

Several aspects were modified of the routine procedures⁵ used in our laboratory for the determination of SIMS U-Pb zircon in order to achieve the precise U-Pb age at a scale of $<5 \mu\text{m}$. Firstly, the Gaussian illumination mode of the primary beam was used instead of the Köhler mode which is used for routine analysis. Secondly, the primary beam intensity was reduced to *ca.* 100 pA, which is only *ca.* 1–2% of that used in the routine analysis. Thirdly, with a small primary beam size, we were able to use higher magnification transfer settings than those used in routine analysis to maximize the secondary transmission and improve the analytical precision. We address the relevant modifications in detail below.

3.1 Primary beam settings

Two illumination modes, the Köhler mode and Gaussian mode, can be used in the large-geometry CAMECA ims-1270/1280 SIMS. The Köhler illumination consists of the upstream lenses for illuminating an aperture and the last lens of the primary column for producing an image of this aperture onto the target surface with a uniform beam density. The beam size

under the Köhler illumination mode mostly depends on the size of the apertures cutting the primary beam.¹¹ This mode is commonly used for routine U–Pb measurements with a beam size of 10–30 μm . The Gaussian illumination forms a reduced ion source image onto the sample with a focused beam density. Thus, a smaller primary beam with a higher ion density can be achieved. In this study, we use the Gaussian illumination mode to obtain a finely-focused (<5 μm) primary beam. Both O^- and O_2^- were employed as the primary ion species.

The primary ions (mixture of O_2^- and O^-) were accelerated at -13 kV and passed through a Primary Beam Mass Filter (PBMF), which is an electromagnet used for selecting specific mass for the primary beam species (Fig. 1). The O_2^- primary ion was selected by the PBMF in the first session. One of the largest (3 mm) apertures, the 1st Primary aperture (PBMF-Aperture), was used to maximize the primary ion transfer. Then, the beam was focused by Lens 2 and Lens 3, respectively. Finally, the primary beam was cut by a relatively small (200 μm) Last Primary Aperture (Lens 4 Aperture) to reduce aberrations (Fig. 1). Stigmators between the Last Primary Aperture and Lens 4 were carefully tuned to minimize the aberrations. All the deflectors after each electrostatic lens were utilized to center the primary beam and maximize the intensity. The primary beam intensity depends mostly on the voltage of Lens 3.

By controlling the PBMF magnetic field, the O^- ion was alternatively selected as the primary beam species in the second session, with the rest of the instrument settings being similar to those used in the first session. Lens voltages were readjusted to adapt the light O^- ions. Additional tuning of Deflector 1 was performed, because the positions for generating O_2^- and O^- beams in the source are different.

Based on the settings described above, the Gaussian mode primary O_2^- and O^- ions with intensity of ~ 100 pA were used for zircon U–Pb measurements in session 1 and 2, respectively.

3.2 Secondary ion optical settings

The secondary ions were accelerated at a potential of +10 kV, and passed through a set of transfer electrostatic lenses, which were settled to a magnification of ~ 260 between the sample surface and the field aperture to ensure high transmission. Two electrostatic lenses (Lt1 and Lt3) in the transfer section were used to achieve high magnification, with voltages of 30% and 89% of the maximum lens voltage, respectively. After that, the secondary ions were projected on to the field aperture with a width of 6000 μm to balance the high transmission and the sharpness of the entrance slit image. A combination of 55 μm entrance slit and 173 μm exit slit was used to achieve a MRP of *ca.* 7000 (50% peak height), which effectively separates Pb^+ peaks from the isobaric interferences.

After energy dispersion by the ESA, a band-width of 60 eV energy slit was used to reduce the energy dispersion to an acceptable level. Rectangular lenses were activated in the coupling section between the ESA and mass analyzer to enhance secondary ion transmission by compressing the sample image along the y direction.

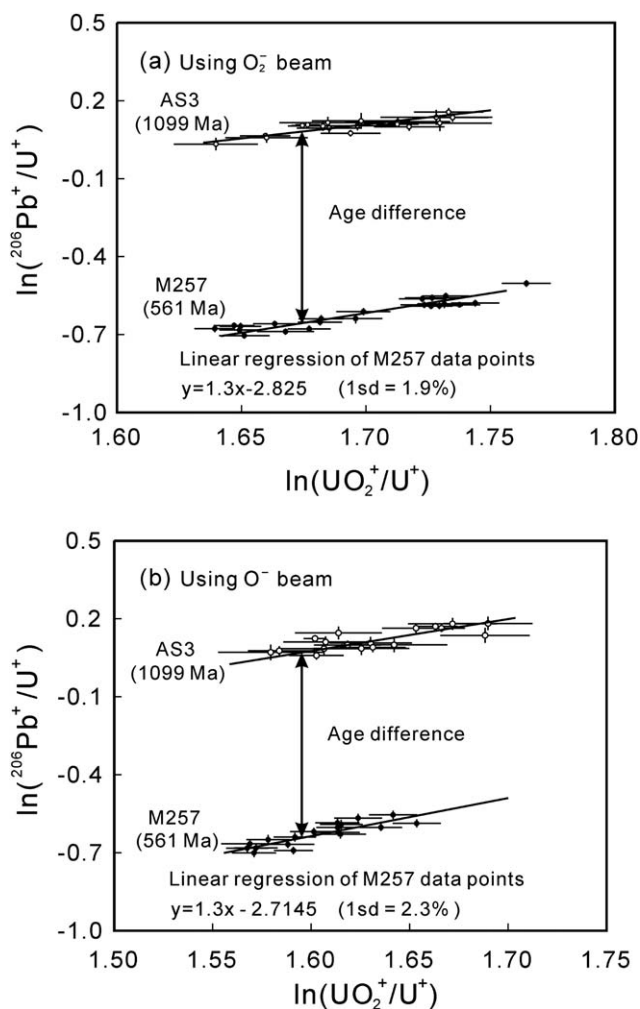


Fig. 2 Logarithmic calibration graphs of $^{206}\text{Pb}^+ / ^{238}\text{U}^+$ vs. $^{270}\text{UO}_2^+ / ^{238}\text{U}^+$ of the M257 zircon as a standard along with AS3 zircon as an unknown in (a) the first and (b) the second session. A calibration slope of 1.3 and two zircons separated in age by 538 million years is shown. The 1σ standard deviation of the Pb/U values of the calibration curve is 1.9% and 2.3% for the first and second session, respectively.

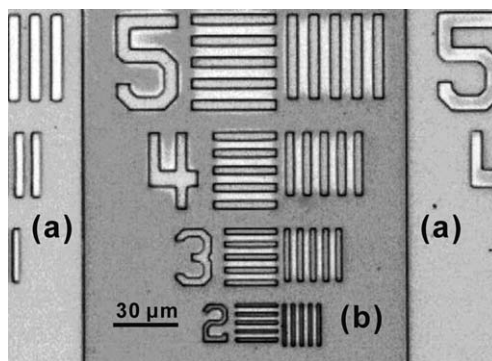


Fig. 3 The standard sample used for estimating the primary beam size. (a) silicon underlay (b) tantalum plate (0.2 μm thick) with etched lines and figures. The etched lines have different gap and bar width ranging from 1 μm to 5 μm .

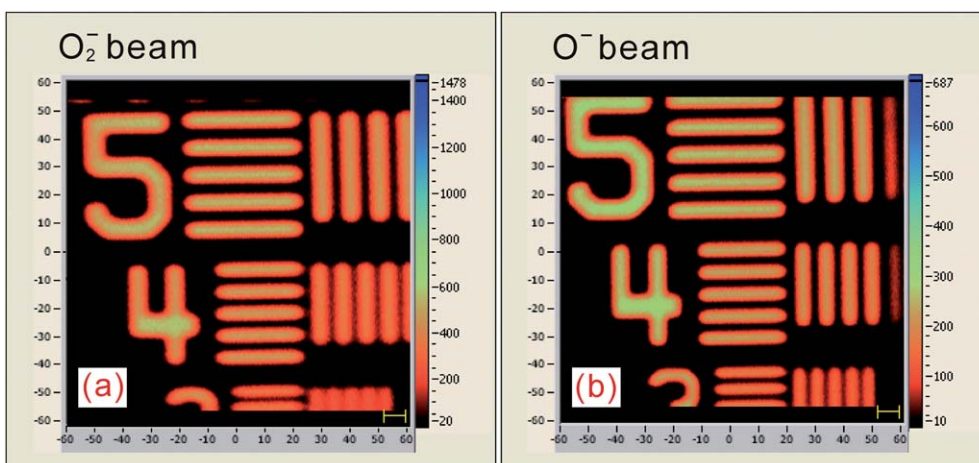


Fig. 4 Secondary ion images of Si^+ obtained from the standard sample. (a) and (b) are images of $120 \mu\text{m} \times 120 \mu\text{m}$ in size showing parallel silicon lines of 3 to $5 \mu\text{m}$ gap obtained by scanning the primary O_2^- and O^- beam in sessions 1 and 2, respectively.

3.3 U–Pb isotope measurements

Three well-characterized international zircon standards (M257,¹² AS3¹³ and Plešovice¹⁴) and our in-house zircon standard (Qinghu⁵) with ages ranging from the Mesoproterozoic to Jurassic were cast in transparent epoxy mounts, which were then polished to section the crystals in half for analysis. The mounts were vacuum-coated with high-purity gold prior to SIMS analysis. The M257 zircon was used as the standard for calibration of U/Pb fractionation and U abundance, while the others were analyzed as unknowns to test the precision and accuracy of U–Pb age at a scale of up to *ca.* $5 \mu\text{m}$ in two sessions: using O_2^- and O^- as primary ion species in sessions 1 and 2, respectively.

A Single Electron Multiplier (EM) was used to measure the secondary ion beam intensities by peak-jumping in sequence: 195.94 ($^{180}\text{Hf}^{16}\text{O}$, high intensity peak for centering the secondary ion beam as well as energy and mass), 199.80 ($^{92}\text{Zr}_2^{16}\text{O}$, reference mass), 200.50 (background of detector), 203.97 (^{204}Pb), 205.97 (^{206}Pb), 206.98 (^{207}Pb), 207.98 (^{208}Pb), 238.05 (^{238}U), 248.03 ($^{232}\text{Th}^{16}\text{O}$), 270.04 ($^{238}\text{U}^{16}\text{O}_2$), with an integration time of 0.56, 1.04, 2.08, 4.16, 6.24, 10.40, 2.08, 4.16, 2.08 and 2.96 s (based on the unit time of 0.08 s), respectively. Each measurement consisted of 15 cycles, with a total analytical time of ~ 20 min.

The oxygen flooding technique¹⁵ (1×10^{-5} Torr in sample chamber) was used to enhance Pb^+ sensitivity to a value of

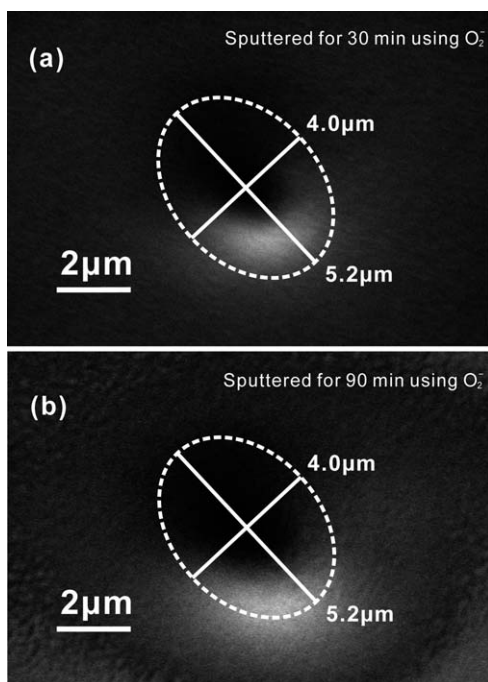


Fig. 5 Secondary electron images of the O_2^- beam crater on zircon sputtered for 30 min (a) and 90 min (b). The spot size was determined to be approximately $5.2 \mu\text{m} \times 4.0 \mu\text{m}$.

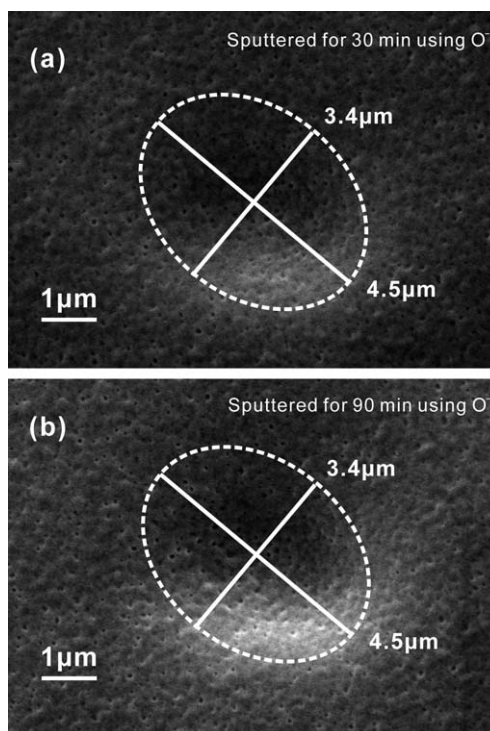


Fig. 6 Secondary electron image of O^- beam crater on zircon sputtered for 30 min (a) and 90 min (b). The spot size was estimated to be $4.5 \mu\text{m} \times 3.4 \mu\text{m}$.

~21 cps/ppm/nA and ~13 cps/ppm/nA by using O_2^- and O^- as primary species, respectively, calculated against the M257 standard zircon.¹² A 200 s pre-sputtering using a 2.5 nA homocentric primary beam (raster 25 μ m) was performed, followed by a 60 s secondary ion beam centering procedure using a 100 pA working beam.

The mass calibration was carried out alternately by using NIST610 glass and M257 zircon standards. Mass peaks of ^{180}Hf ^{16}O and $^{92}\text{Zr}_2^{16}\text{O}$ were centered by using the M257 zircon, while the other peaks were centered by using NIST610. Pb/U fractionation was calibrated according to the power relationship

between $^{206}\text{Pb}/^{238}\text{U}$ and $^{238}\text{U}^{16}\text{O}_2/^{238}\text{U}$.^{5,15} The standard deviations of the Pb/U values of the reference curve were 1.9% and 2.3% in sessions 1 and 2 (Fig. 2), respectively, which were propagated together with the errors from the unknowns to give an overall error for the Pb/U ratio of each analysis. Uncertainties for individual analyses in the data table are reported at a 1σ level; mean ages are quoted with 95% confidence interval by pooling multiple U/Pb and Pb/Pb analyses for the same samples. Data reduction was carried out using the Isoplot/Ex v.3.0 program.¹⁶ Analytical results are presented in ESI Table 1, the sensitivity data are presented in ESI Table 2.† The ^{204}Pb counting rate is

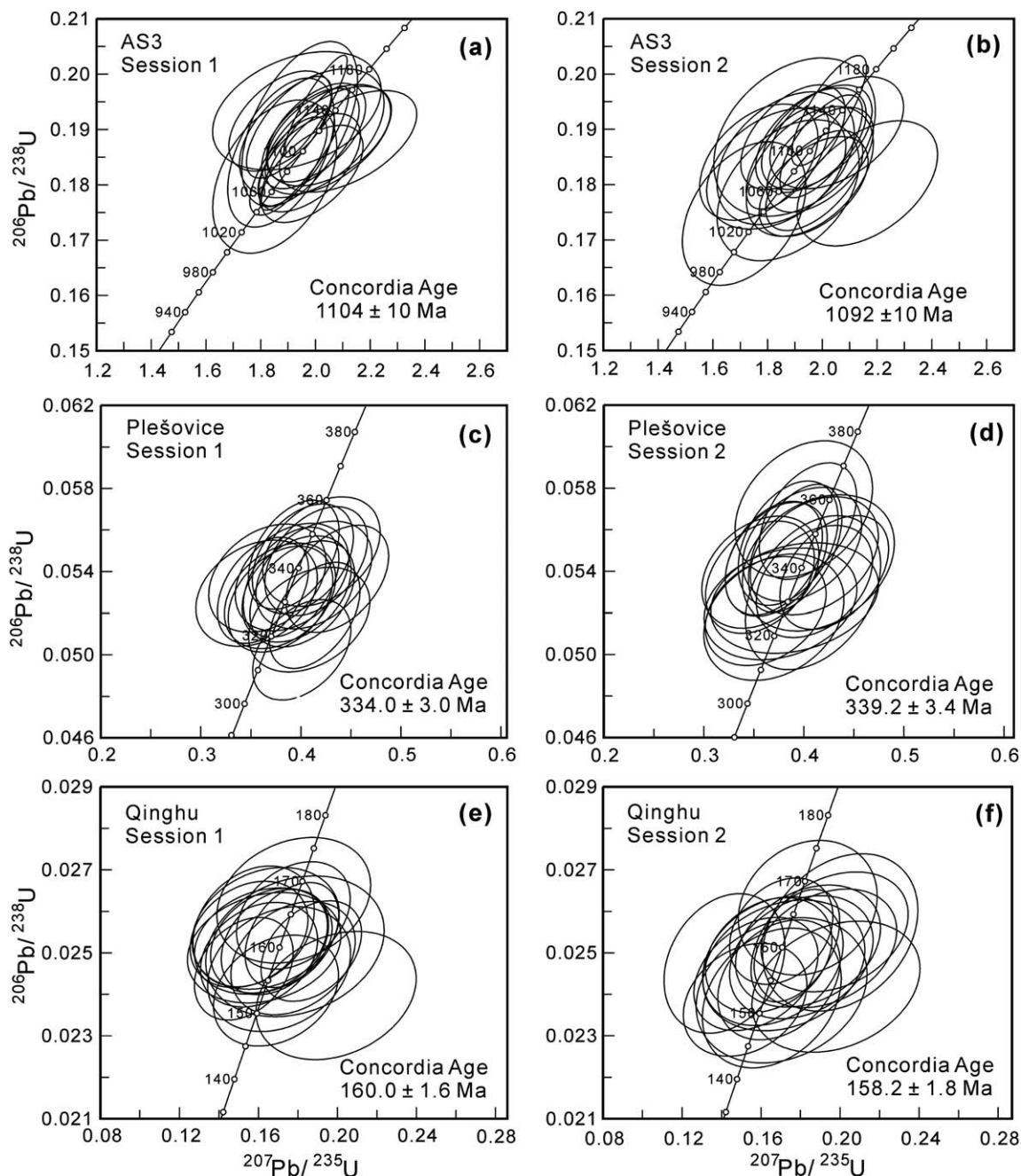


Fig. 7 U–Pb zircon concordia diagram for AS3 (a–b), Plešovice (c–d) and Qinghu (e–f). Gaussian mode primary O_2^- and O^- beams with intensity of ~100 pA were used in sessions 1 and 2, respectively. Data-point error ellipses are 2σ .

below the detection limit (<0.01 cps) for the measurement, thus the ^{208}Pb method³ was alternatively used for common lead correction. During the experiment, the minimum spot-to-spot distance was 40 μm to ensure similar charging conditions on each spot.

4. Results

4.1 Lateral resolution

For the Gaussian mode primary beam, the lateral resolution is defined as the minimum distance of two spots (area) on the sample surface corresponding to signal levels of 16 and 84 percent using a knife-edge sample (*e.g.*, ref. 17–19). However, the knife-edge method is time-consuming and requires specific samples.⁶ Alternatively, the primary beam size can be either determined by Scanning Ion Imaging (SII) with the SIMS, or estimated by examining secondary electron (SE) images of the sputtered crater using a Scanning Electron Microscope (SEM).⁶

By scanning the primary beam (O_2^- or O^-) on the standard sample (Fig. 3) and detecting the $^{28}\text{Si}^+$ signal using the ion probe mode of the SIMS, we obtained the SII images by using O_2^- (Fig. 4a) and O^- (Fig. 4b). The $^{28}\text{Si}^+$ signal can be detected where the tantalum plate is pierced. Primary beam size can be estimated on the basis of the image definition (sharpness of the bars). The smaller the beam size, the better the image definition. During the first session using ~ 100 pA O_2^- , an image with clear-cut 5 μm vertical parallel lines and 4 μm horizontal parallel lines were obtained (Fig. 4a), indicating that the primary O_2^- beam is about 5 μm in the x -direction and about 4 μm in the y -direction. Similarly, a ~ 100 pA primary O^- beam was used to scan an SII image (Fig. 4b) on the same sample during the second session. The beam size was estimated at 4 μm and 3 μm in the x and y directions, respectively.

Secondary electron images of the craters on the zircon surface, which were sputtered for 30 min and 90 min by O_2^- (Fig. 5a, b) and by O^- (Fig. 6a, b) in sessions 1 and 2, respectively, were also used to determine the spot size. The boundary of the craters sputtered by O^- can be easily defined due to the clarity of the image. The O^- beam size was determined at 4.5 $\mu\text{m} \times 3.4$ μm (Fig. 6a, b) based on the size of the half bright region.⁶ As for the O_2^- craters shown in Fig. 5a and 5b, the crater boundary is unclear due to the shallowness of the crater and the smoothness of the surface. The O_2^- beam size was determined to be approximately 5.2 $\mu\text{m} \times 4.0$ μm based on the brightness distribution of the image.

4.2 U–Pb zircon ages

4.2.1 AS3 zircon. The AS3 zircon comes from the anorthositic series of mafic rocks in the composite Mesoproterozoic Duluth complex of northeastern Minnesota,¹³ and has been used as the SIMS U–Pb zircon age standard by a number of high resolution SIMS laboratories. This zircon is precisely dated at 1099.1 \pm 0.2 Ma by isotope dilution thermal ionization mass spectrometry (ID-TIMS).^{13,20}

Eighteen measurements of U–Pb isotopes were conducted on AS3 zircon in the first session by using an O_2^- beam. All the analyses are concordant within analytical errors (Fig. 7a). The common lead was low (f_{206} was <0.4%). A concordia age was

calculated at 1104 \pm 10 Ma. In the second session, using the O^- beam, eighteen additional spots were measured. The value of f_{206} was <0.2%. All the analyses are concordant, yielding a concordia age of 1092 \pm 10 Ma (Fig. 7b). Therefore, the concordia ages obtained in both sessions are in agreement within errors with the reference value of 1099 Ma.

4.2.2 Plešovice zircon. Plešovice zircon comes from a potassic granulite facies rock at the Plešovice quarry in the southern Bohemian Massif, Czech Republic. It is concordant in the U–Pb isotopic system, with a weighted mean $^{206}\text{Pb}/^{238}\text{U}$ age of 337.1 \pm 0.4 Ma dated by ID-TIMS.¹⁴

Eighteen analyses were carried out in each O_2^- and O^- session. The value of f_{206} was <0.3%. The results are all concordant within analytical errors, yielding a concordia age of 334.0 \pm 3.0 Ma and 339.2 \pm 3.4 Ma in sessions 1 and 2, respectively (Fig. 7c, d). Thus, the U–Pb results obtained in the two sessions agree well within errors with the reference value.

4.2.3 Qinghu zircon. The Qinghu zircon was separated from a felsic syenite rock at a large quarry in the Qinghu alkaline complex near the border between Guangdong and Guangxi Provinces of South China. It has concordant U–Pb ages and homogeneous hafnium and oxygen isotopes,^{5,21} and is served as an in-house U–Pb age standard with 159.5 \pm 0.2 Ma dated by ID-TIMS.⁵

Eighteen analyses were carried out in each session. The value of f_{206} was <0.6%. The results are all concordant within analytical errors, yielding a concordia age of 160.0 \pm 1.6 Ma and 158.2 \pm 1.8 Ma in sessions 1 and 2, respectively (Fig. 7e, f). Therefore, the U–Pb results obtained in the two sessions are indistinguishable within errors from the TIMS date.

5. Concluding remarks

The results presented above indicate that the CAMECA ims-1280 SIMS is capable of determining zircon U–Pb ages as young as the Jurassic at ~ 5 μm scale using the Gaussian illumination O_2^- or O^- primary beam. A precision and accuracy of 1–2% can be achieved by pooling 15–20 repeat measurements, comparable with the routine SIMS analysis using the Köhler illumination primary beam at *ca.* 10–30 μm scale. Our good results have also benefited greatly from the optimized high transmission secondary optical system of the CAMECA ims-1280 SIMS.

While the Köhler illumination beam is primarily used for routine SIMS U–Pb measurements at a scale of *ca.* 10–30 μm (as it produces a flat bottom crater on the target surface), it is not feasible for use at a scale of 5 μm or less because of its low current density as well as mechanical difficulties. To achieve a high lateral resolution at 5 μm scale or less, the Gaussian illumination primary beam has significant advantages because of its focused current density. Despite a “V-shaped” crater on the target surface produced by the Gaussian illumination primary beam, the depth of the crater is only *ca.* 500 nm, it is very shallow due to the low intensity of the primary beam (*ca.* 100 pA) and the short sputtering time (*ca.* 20 min). This shallow crater has negligible influence on the variation of U/Pb fractionation.

The sensitivity obtained for the measurement of secondary Pb^+ in zircon is lower when the O^- beam is used compared with that obtained with the O_2^- primary beam, *i.e.* ~ 21 cps/ppm/nA using

O₂⁻ vs. ~13 cps/ppm/nA using O⁻, resulting in a slightly poorer precision for single spot measurement. However, pooled analyses of 15–20 U/Pb measurements using the O⁻ beam can yield a U–Pb age precision and accuracy comparable with those obtained using the O₂⁻ beam. More importantly, the O⁻ beam has a higher density than the O₂⁻ beam, producing a smaller crater on the target surface with a given 100 pA beam current. Therefore, the O⁻ primary beam is preferably used for U–Pb zircon age determination at a scale of down to <5 μm. On the other hand, for U-poor minerals with younger ages, it might be preferable to use the O₂⁻ primary beam to generate sufficient secondary ions of Pb for precise measurement.

Acknowledgements

We thank Sláma, J. and Liu, D.Y. for providing Plešovice and M257 zircon standards, respectively. QZY thanks Kevin McKeegan for his generosity by literally “pouring out AS3 gems out of his treasure box”. The paper has benefited from constructive reviews by an anonymous referee. This work was supported by the State Key Laboratory of Lithospheric Evolution, IGG-CAS (Grants Z201003 and Z0908).

References

- 1 T. R. Ireland and I. S. Williams, *Rev. Mineral. Geochem.*, 2003, **53**, 215–241.
- 2 C. A. Andersen and J. R. Hinthorne, *Earth Planet. Sci. Lett.*, 1972, **14**, 195–200.
- 3 W. Compston, I. S. Williams and C. Meyer, *J. Geophys. Res.*, 1984, **89**, B525–B534.
- 4 W. Compston and S. W. J. Clement, *Appl. Surf. Sci.*, 2006, **252**, 7089–7095.
- 5 X. H. Li, Y. Liu, Q. L. Li, C. H. Guo and K. R. Chamberlain, *Geochem., Geophys., Geosyst.*, 2009, **10**, Q04010, DOI: 10.1029/2009GC002400.
- 6 R. A. Stern, I. R. Fletcher, B. Rasmussen, N. J. McNaughton and B. J. Griffin, *Int. J. Mass Spectrom.*, 2005, **244**, 125–134.
- 7 A. K. Schmitt, K. R. Chamberlain, S. M. Swapp and T. M. Harrison, *Chem. Geol.*, 2010, **269**, 386–395.
- 8 K. R. Chamberlain, A. K. Schmitt, S. M. Swapp, T. M. Harrison, N. Swoboda-Colberg, W. Bleeker, T. D. Peterson, C. W. Jefferson and A. K. Khudoley, *Precambrian Res.*, 2010, **183**, 379–387.
- 9 M. Grove and T. M. Harrison, *Geology*, 1999, **27**, 487–490.
- 10 S. J. Mojzsis and T. M. Harrison, *Earth Planet. Sci. Lett.*, 2002, **202**, 563–576.
- 11 T. R. Ireland, in *Handbook of Stable Isotope Analytical Techniques*, ed. A. d. G. Pier, Elsevier, Amsterdam, 2004, pp. 652–691.
- 12 L. Nasdala, W. Hofmeister, N. Norberg, J. M. Martinson, F. Corfu, W. Dörr, S. L. Kamo, A. K. Kennedy, A. Kronz, P. W. Reiners, D. Frei, J. Kosler, Y. Wan, J. Götze, T. Häger, A. Kröner and J. W. Valley, *Geostand. Geoanal. Res.*, 2008, **32**, 247–265.
- 13 J. B. Paces and J. D. Miller Jr., *J. Geophys. Res.*, 1993, **98**, 13997–14013.
- 14 J. Sláma, J. Košler, D. J. Condon, J. L. Crowley, A. Gerdes, J. M. Hanchar, M. S. A. Horstwood, G. A. Morris, L. Nasdala, N. Norberg, U. Schaltegger, B. Schoene, M. N. Tubrett and M. J. Whitehouse, *Chem. Geol.*, 2008, **249**, 1–35.
- 15 Q. L. Li, X. H. Li, Y. Liu, G. Q. Tang, J. H. Yang and W. G. Zhu, *J. Anal. At. Spectrom.*, 2010, **25**, 1107–1113.
- 16 K. R. Ludwig, Berkeley Geochronology Center, 3.0 edn 2003, p. Spec. Pub 4.
- 17 H. Arimoto, A. Takamori, E. Miyauchi and H. Hashimoto, *Jpn. J. Appl. Phys.*, 1983, **22**, L780–L782.
- 18 M. Grasserbauer, K. F. J. Heinrich and G. H. Morrison, Nomenclature, symbols and units recommended for *in situ* microanalysis, *Pure Appl. Chem.*, 1983, **55**, 2023–2027.
- 19 M. Senoner and W. E. S. Unger, *Surf. Interface Anal.*, 2007, **39**, 16–25.
- 20 M. D. Schmitz, S. A. Bowring and T. R. Ireland, *Geochim. Cosmochim. Acta*, 2003, **67**, 3665–3672.
- 21 X. H. Li, W. X. Li, X. C. Wang, Q. L. Li, Y. Liu and G. Q. Tang, *Sci. China Ser. D*, 2009, **52**, 1262–1278.